ACS OMEGA

Open Access

http://pubs.acs.org/journal/acsodf

Article

N-Salicyl-AA$_n$-picolamide Foldameric Peptides Exhibit Quorum Sensing Inhibition of *Pseudomonas aeruginosa* (PA14)

Subhashree S. Panda, Supriya Kumari, Manjusha Dixit, and Nagendra K. Sharma*

Cite This: *ACS Omega* 2023, 8, 30349−30358

Read Online

ACCESS | Metrics & More | Article Recommendations | Supporting Information

ABSTRACT: An organic acid, salicylic acid, and its derivatives are constituents of various natural products possessing remarkable bioactivity. *O*-Acetyl salicylate (aspirin) is a well-known life-saving drug. Its peptide derivative salicylamide has also been explored in the designing of peptide-based therapeutic drugs. An organic base, picolylamine has been recently explored for designing diagnostic probes. However, both the acid and base have common features as metal chelating with coordinating metals. Thus, these scaffolds could be used for designing inhibitors of various metalloenzymes. Their characteristic properties encourage us to design peptides containing both scaffolds (salicylic acid and picolylamine) at opposite terminals. So far there is no report available on such conjugated peptides. This report describes the synthesis, conformational analysis, and biochemical assessment of rationally designed *N*-salicyl-AA$_n$-picolamide peptides. Pleasantly, we have obtained the crystal structures of representative peptides that confirm their roles in conformational changes. Our biological assessment as quorum sensing inhibitors has revealed that their di/tripeptides inhibit quorum sensing of the pathogenic bacterium PA14 strain. Hence, these peptides have promising foldameric and therapeutic values.

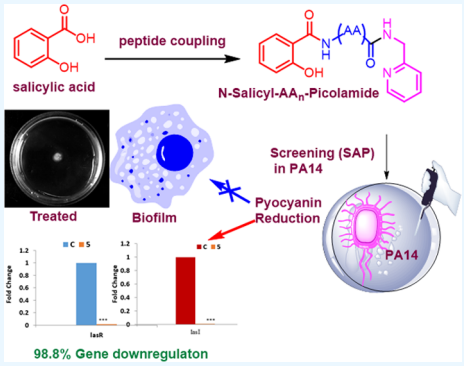

INTRODUCTION

Salicylic acid and its derivatives are constituents of various natural products comprising the phenolic group with numerous therapeutic effects.[1] The simplest derivative, O-acetyl salicylate, also known as aspirin, is a nonsteroidal anti-inflammatory drug (NSAID).[2] Salicylic acid-conjugated amino acids/peptides are also explored in the development of novel drug candidates. The amide derivatives of salicylic acid, salicylamide (SAM), possess analgesic and antipyretic properties.[3] Salicylamide is also considered as a potential scaffold for designing therapeutic peptide drugs by altering the peptide structure and conformation.[4,5] Deng has synthesized novel salicylamide derivatives which show selective Ache inhibition, antioxidant features, Ab-aggregation, anti-neuroinflammation, and BBB permeability, a potential drug of Alzheimer's disease.[6] The *N*-salicylic-dipeptides inhibit human platelet aggregation, which is induced by collagen, ADP, and adrenaline.[7] However, RGD analogues containing salicylic acid derivatives show antiplatelet activities.[8] De Grado has used salicylic acid for novel self-assembling foldamers that inhibit heparin−protein interactions.[9] Zeng has synthesized foldable aromatic oligoamides comprising a salicylic acid moiety which form helical structures through continuous hydrogen bonding.[10,11] Imramovsky has synthesized benzamide derivatives of *N*-salicylate amino acid molecules that induce apoptosis in cancer cell lines.[12] A very few picolylamine containing peptides are reported and employed for the chelation with metal ions.[13−16] In the literature, salicylic acid and its derivatives exhibit antibacterial properties by inhibiting the quorum sensing (QS) system of pathogenic bacteria.[17] QS is a bacterial cell−cell communication process that involves the production, detection, and response to extracellular signaling molecules.[18] In general, Gram-positive and Gram-negative bacteria use QS communication circuits to regulate their various physiological activities such as symbiosis, virulence, competence, conjugation, antibiotic production, motility, sporulation, and biofilm formation.[19] To control bacterial infections, drug-design strategies have been advanced by aiming the inhibition of the virulence factors against designing the complete bactericidal drugs (QS inhibitors). Nowadays, antibiotic drug-design strategies have been changed to find a sustainable solution to counteract the multidrug resistance issue.[20] A multidrug-resistant and highly adaptable bacterium is responsible for nosocomial infections. The pathogenic bacterium *Pseudomonas aeruginosa* (PA) is also a multidrug-resistant and highly adaptable bacterium which is responsible for nosocomial infections[21] and a prime concern for hospital-acquired infections in European countries.[22] The persistent use of antibiotics has significantly reduced mortality but, at the same time, become the leading cause for the emergence of

Received: May 19, 2023
Accepted: July 26, 2023
Published: August 8, 2023

Scheme 1. Synthesis of Salicylic Acid and Picolylamine-Conjugated Peptides

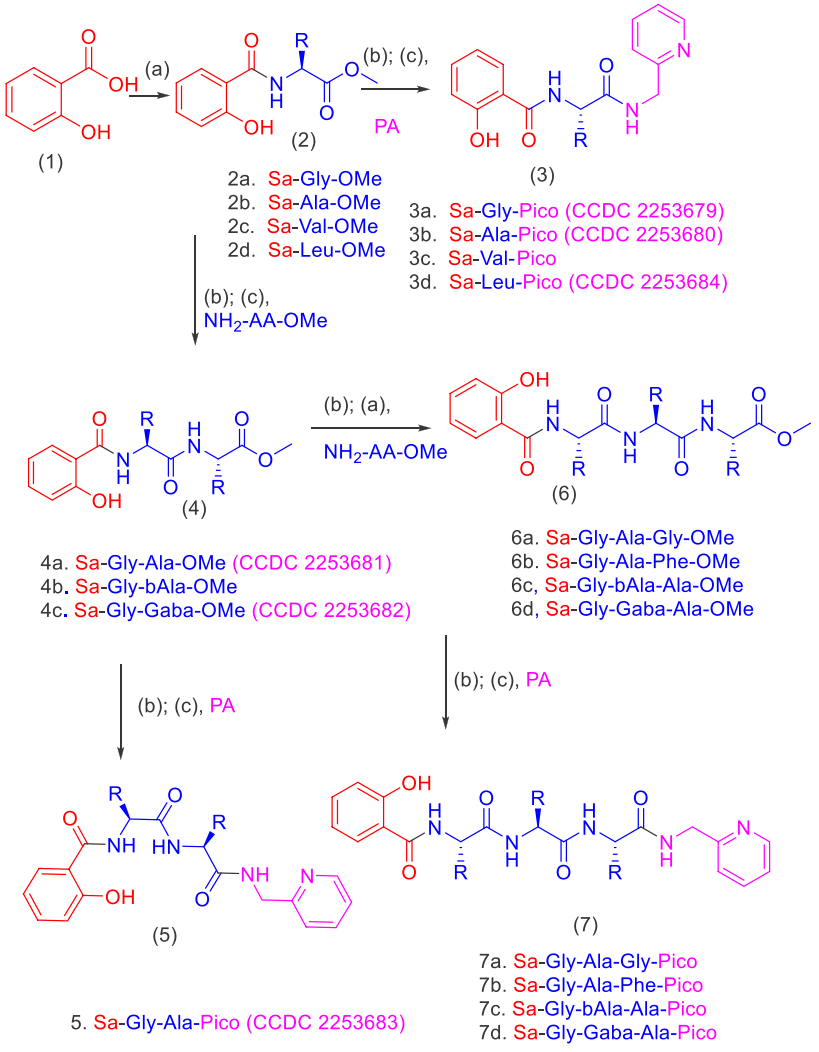

antibiotic-resistant bacterial pathogenic strains.[23] Recently, our group has also explored nonbenzenoid derivatives, aminotroponyl sulfones, as anti-QS inhibitors.[24] In the repertoire of salicylic acid−picolylamin-conjugated peptides, we have rationally designed novel peptides *N*-salicyl-AA$_n$-picolylamine to evaluate their role in the structural folding and therapeutic values. This report describes their synthesis, conformational analyses, and QS inhibition studies in PA14.

RESULTS AND DISCUSSION

We derivatized salicylic acid (**1**) into N-salicyl-amino acid ester derivatives, Sa-AA-OMe (**2**), under amide bond coupling reaction conditions (Scheme 1). At this stage, the nonpolar amino acids ester derivatives (glycine, alanine, valine, and leucine) were employed to prepare the respective Sa-AA-OMe (**2a−2d**). These derivatives were conjugated with picolylamine in two steps (hydrolysis of ester and amide coupling), which produced rationally designed picolylamine-conjugated dipeptides, Sa-AA-Pico (**3a−3d**). We also synthesized salicyl dipeptides, Sa-AA$_2$-OMe (**4a−4d**), and salicyl tripeptides, Sa-AA$_3$-OMe (**6a−6d**), to use as a spacer between picolylamine and salicylic acid. Subsequently, these peptides were conjugated with picolylamine and converted into the desired peptides Sa-(AA)$_n$-Pico (**5** and **7**) under amide coupling conditions. The characterization data (NMR and HRMS) of all new products are provided in the Supporting Information (SI).

For structural and conformational studies, we attempted to crystallize those peptides and obtained the single crystals of **3a**, **3b**, **3d**, and **5** in DCM/MeOH (1:1). Their solved data are submitted to the Cambridge Crystallographic Data Centre (CCDC). Their reference numbers are 2253679−2253684, which also describe concerning compounds. Their structural refinement parameters are provided in the SI. Carefully, we prepared their packing diagram from the respective crystal X-ray data and explored the role of salicylic acid/picolylamine scaffolds in the structural organization of novel peptides through noncovalent interactions. The peptide Sa-Gly-Pico (**3a**) forms a three-dimensional cross-linked supramolecular structure through the intermolecular H-bonding with the bond distance of 2.1 Å, owing to the amide groups in both fashions, parallel horizontally and antiparallel vertically (Figure 1A). In addition, its salicylic residue has intramolecular hydrogen

https://doi.org/10.1021/acsomega.3c03404
ACS Omega 2023, 8, 30349−30358

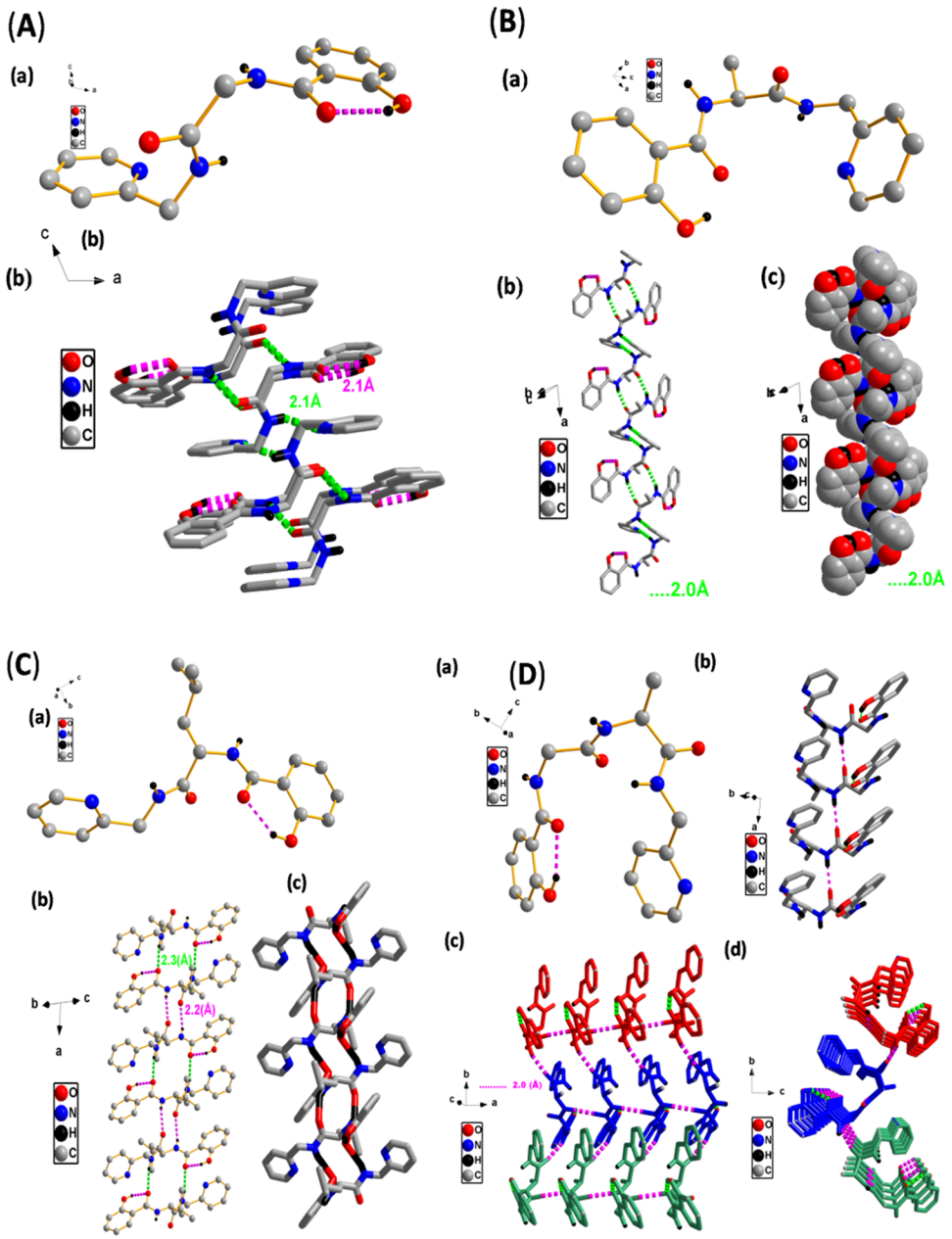

Figure 1. Crystal structure and packing diagram of peptides: (A) structure of **3a** (a) and its packing diagram (b), (B) structure of peptide **3b** (a) and its packing diagram (b–c), (C) structure of peptide **3d** (a) and its packing diagram (b–c), and (D) structure of peptide **5** (a) and its packing diagram (b–d).

bonding. The peptide *Sa-Ala-Pico* (**3b**) forms a novel supramolecular helical structure through hydrogen bonding between amide groups at a distance of 2.0 Å (Figure 1B). The peptide *Sa-Leu-Pico* (**3d**) forms a ladder-type supramolecular structure because of intermolecular hydrogen bonding between two antiparallel molecules with a distance of 2.3 Å (Figure 1C). Its salicylic acid residue also has intramolecular hydrogen bonding. The peptide *Sa-Gly-Ala-Pico* (**5**) has folded structure and forms unique supramolecular helical structures owing to the intermolecular hydrogen bonding through amide groups. Two consecutive helices are also joined by another set of hydrogen bonding with a bond distance of 2.0 Å (Figure 1D). In addition, its salicylic acids also exhibit intramolecular hydrogen bonding.

We also obtained the crystal structures of salicyl peptides without containing picolylamine (**4a**/**4c**) in $CDCl_3$. Their structure and packing diagrams are depicted in Figure 2, while other X-ray parameters are provided in the Supporting Information. The crystal structure of the Sa-α-peptide (**4a**) forms a unique cylindrical supramolecular structure with a diameter of ∼4.5 Å through intermolecular hydrogen bonding (∼2.1 Å) owing to the amide groups such as N−H···O═C in the antiparallel orientation (Figure 2A). The Sa-α-γ-peptide (**4c**) forms a supramolecular β-sheet-type structure owing to the intermolecular hydrogen bonding in its antiparallel amide groups with a distance of 2.0 Å. In addition, salicylic phenolic residue also forms intermolecular H-bonds (1.8 Å) with parallel amide carbonyl molecules (Figure 2B).

https://doi.org/10.1021/acsomega.3c03404
ACS Omega 2023, 8, 30349−30358

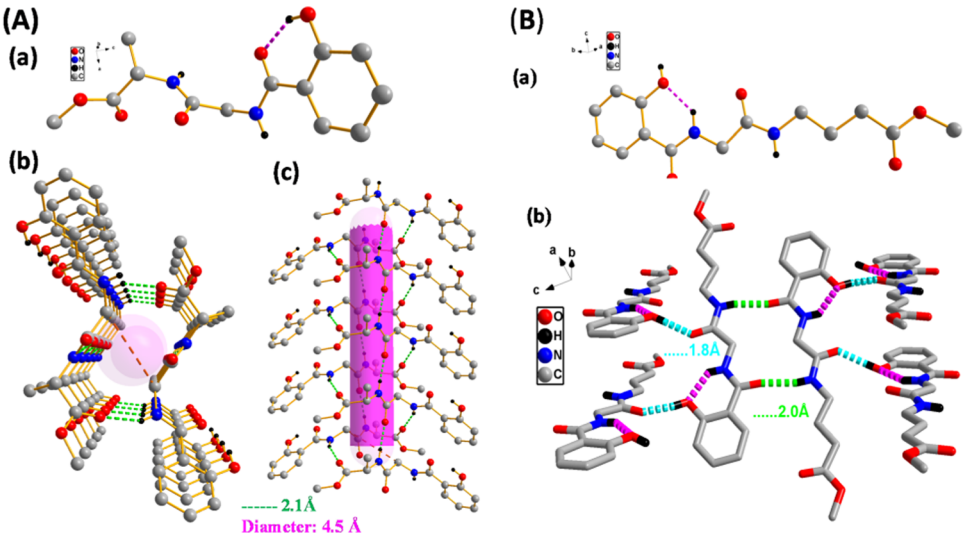

Figure 2. Crystal structure and packing diagram of peptides: (A) structure of **4a** (a) and its packing diagram (b−c) and (B) structure of peptide **4c** (a) and its packing diagram (b).

Herein, we attempted to find the conformation of peptides (**3**/**5**/**7**) in the solution phase by 1D/2D-NMR techniques. We recorded 2D-NMR of peptides **3a**−**3d** in CDCl3 and of peptides **5**/**7a**−**7d** in DMSO-d_6. We assigned their chemical shifts from respective 2D-COSY spectra and then extracted their NOE connectivity from respective 2D-NOESY spectra (see the Supporting Information). We noticed strong NOE peaks including the aromatic ring/amide protons that helped to propose the possible conformations as a unique foldamer (Figures S41−S58). Next, we performed ^{1}H NMR DMSO-d_6 titration experiment for finding the intramolecular hydrogen bonding owing to amide N−H's of the chloroform ($CDCl_3$)-soluble peptides (**3a**−**3d**) and generated their titration profiles (δ (ppm) vs $V_{DMSO\text{-}d6}$ in μL) (Figures 3A and S59−S62). In peptide **3a**, we noticed marginal downfield shifts (in ppm) of picolylamide N−H (∼0.5 in **3a**, ∼0.5 in **3b**, and ∼0.2 in **3c**/**3d**) and amino acid amide N−H (∼1.0 in **3a**, ∼0.5 **3b**, ∼0.3 in **3c**, and ∼0.2 in **3d**). In the literature,[25,26] the lower value of chemical shift change indicates the stronger intramolecular hydrogen bonding in $CDCl_3$. Our result supports that amino acid residues have significant roles in the intramolecular hydrogen bonding ability of their amide N−H. Hence, Sa-AA-Pico peptides (**3a**−**3d**) form a stable folded structure in $CDCl_3$ owing to the intramolecular hydrogen bonding.

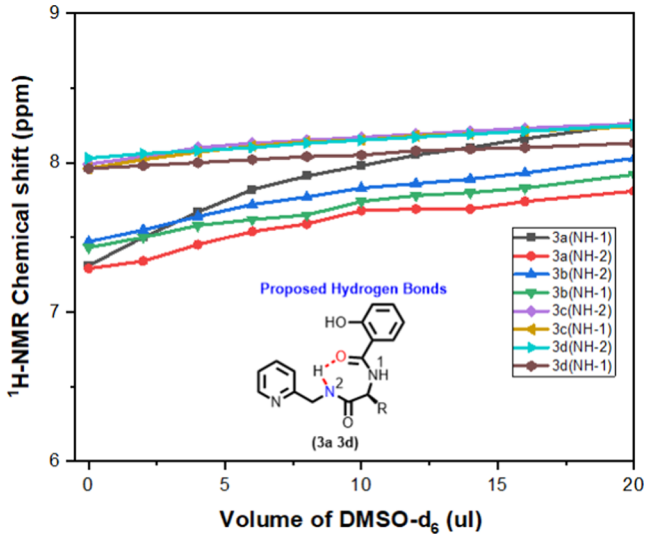

Figure 3. DMSO-d_6 titration NMR profile of peptides **3a**−**3d**.

We noticed that tetrapeptides **7a**−**7d** are soluble only in the DMSO solvent. Thus, we attempted to optimize their structure theoretically using MMFF94 and to find energetically favorable conformation by GMMX. Their energy plots show various possible conformations, which are provided in the SI (Figures 4 and S75−S78). Peptide **7a** shows intramolecular hydrogen bonding (N−H···O═C; O···H−O═C) and $\pi-\pi$ interactions between picolylamide and salicylate aromatic rings at 3.9 Å (Figure 4A). Contrastingly, peptide **7b** exhibits only intramolecular hydrogen bonding, no such $\pi-\pi$ interactions owing to the bulky amino acid residue phenyl alanine. However, the pyridine ring of **7b** exhibit hydrogen bonding with salicylic O−H as N−H···O (Figure 4B). The lowest energy conformer of peptides **7c** and **7d** also exhibits intramolecular hydrogen bonding and $\pi-\pi$ interactions though their hydrogen donors and acceptors are partially altered. Hence salicyl-picolamide-conjugated peptides have a strong ability to form unique foldamers.

The swarming motility and biofilm formation of PA14 reduces the efficacy of drug penetrating ability into the cell walls. These virulent factors and their capacity to conquer antibiotics are controlled by the complex cell to cell chemical signaling system, also known as quorum sensing (QS).[27,28] We treated bacterium PA14 with peptides (**3a**−**3d**/**5**/**7a**−**7d**) and examined swarming of bacterial cells. In comparison to control studies, only peptides **3c** and **5** significantly reduced swarming, despite affecting the bacteria's growing ability even with 100 μM (Figures 5A and S69). Thus, peptides **3c**/**5** are potential antiquorum sensing agents. The QS system is also the key regulator of biofilm formation in the bacterium PA14 strain. We performed an initial screening of those peptides (**3a**−**3d**/**5**/**7a**−**7d**) at a higher concentration (100 μM) to evaluate the biofilm formation activity in the PA14 strain and compared it with the control. Importantly, only two peptides **3c**/**5** remarkably suppressed the biofilm formation in PA14. Then, we performed concentration-dependent biofilm formation in

https://doi.org/10.1021/acsomega.3c03404
ACS Omega 2023, 8, 30349−30358

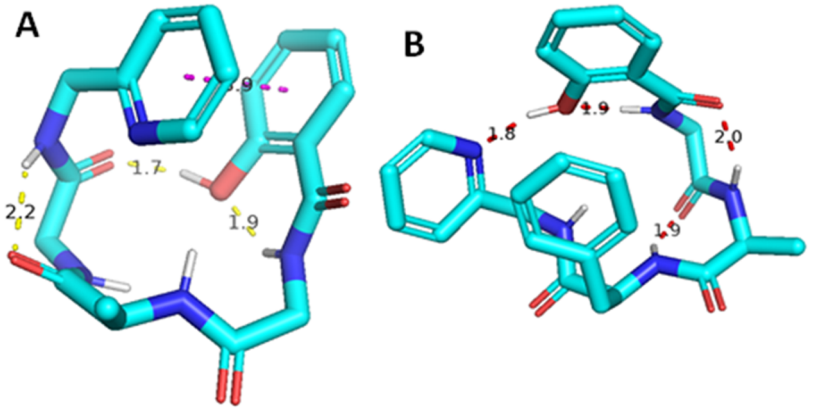

Figure 4. Conformation of the theoretically minimized structure using MMFF94 and GMMX of peptides (A) **7a** and (B) **7b**.

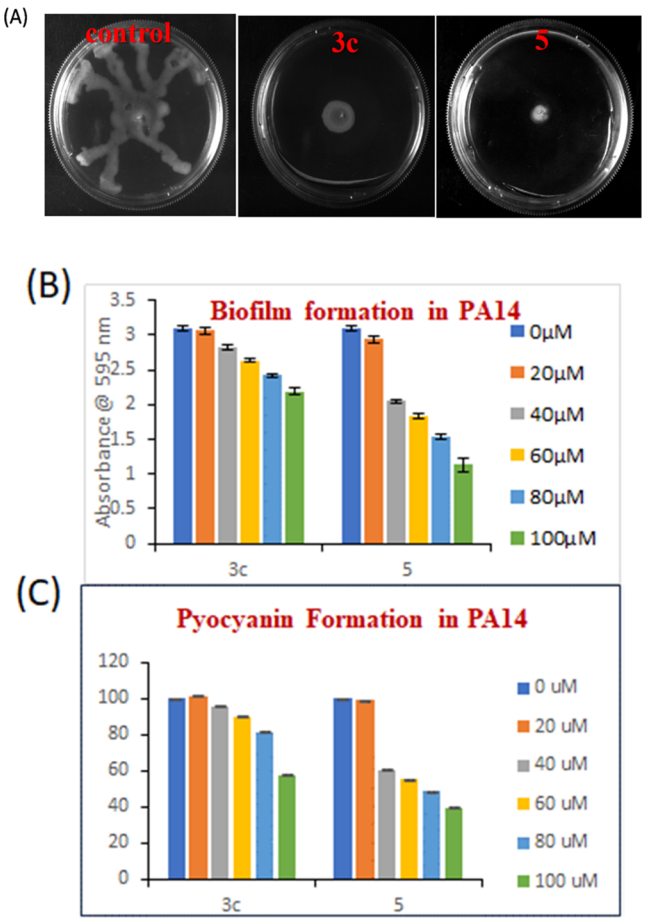

Figure 5. (A) Swarming images of PA14 in the DMSO control and the presence of compounds (**3c** and **5**) at 100 μM concentration, (B) dose-dependent biofilm formation for control and peptides (**3c** and **5**), and (C) dose-dependent pyocyanin production of peptides **3c** and **5**.

the same bacterial strain with those two peptides (**3c**/**5**). Their biofilm activities are provided as a bar diagram (Figure 5B). Our experimental results show that peptides **3c** and **5** suppressed the biofilm formation most effectively at a low concentration of ~40 μM. In the QS system, pyocyanin is a redox-active secondary metabolite phenazine compound that has been considered as both a virulence factor and a quorum sensing signaling molecule in bacterium *P. aeruginosa*.[29] The production of pyocyanin indicates the pathogenicity and sustaining fitness of PA14 in a competitive environment. Thus, we examined the impact of synthetic peptide derivatives (**3a−3d**/**5**/**7a−7d**) on pyocyanin production in the PA14 strain. However, only two peptides (**3c**/**5**) exhibit a significant reduction of the pyocyanin synthesis ($p < 0.001$) at 100 μM. Next, we performed a pyocyanin production assay in a dose-dependent manner and summarized in a bar diagram (Figure 5C). Our result shows that peptide **5** has inhibited the pyocyanin synthesis by 39.18% at 40 μM while 60% at 100 μM.

In the literature, the lasI/R QS circuit regulates the expression of virulent factors.[30] lasR is a transcriptional activator, while lasI regulates the production of the autoinducer N-(3-oxododecanoyl) homoserine lactone (PAI-1).[31] lasR and PAI-1 are required for the induction of lasB (encoding elastase) and other virulence genes. Elastase formation, one of the most virulent characteristics of PA, is the primary cause of PA-mediated death in hospitals. Elastase hydrolyzes internal peptide bonds found on the amino part of hydrophobic amino acid residues, allowing it to cleave a diverse spectrum of proteinaceous substrates. Thus, we conducted a qRT-PCR experiment to assess the effectiveness of synthesized peptide derivatives **3c** and **5** at the gene level. The transcript levels of the 16S RNA gene were similar in control (cells grown LB medium) or in LB medium supplemented with the mentioned peptide, hence it was used for normalization. The compound **5** downregulated lasI and lasR significantly by 98.8% at 40 μM concentration (Figure 6A,B). Interestingly, compound **3c** had no impact on both targeted genes (lasI and lasR), while significantly reducing biofilm formation, pyocyanin production, and swarming motility. The same expression pattern was observed in lasB in the presence of compound **5** (SI, Figure S72). Next, we performed a cytotoxicity experiment in HEK239T cell lines for ensuring the safe usage of synthesized peptides as anti-QS drugs to combat PA14 infection in the human body (SI, Figure S73). We could not notice any significant cytotoxicity at optimal concentration, significantly greater than their anti-QS concentration. Further, to examine the virulence effect of *P. aeruginosa* in cells, another cytotoxicity assay was performed using our synthesized peptide derivative as a therapeutic agent against PA14. PA14 was found to be cytotoxic against the HEK293T cell line, significantly reducing viability when compared to the DMSO control. Their data are summarized in a bar diagram (Figure 6C). This result indicates that compound **5** significantly reduced PA14 virulence-mediated cytotoxicity toward HEK293T cells and

https://doi.org/10.1021/acsomega.3c03404
ACS Omega 2023, 8, 30349−30358

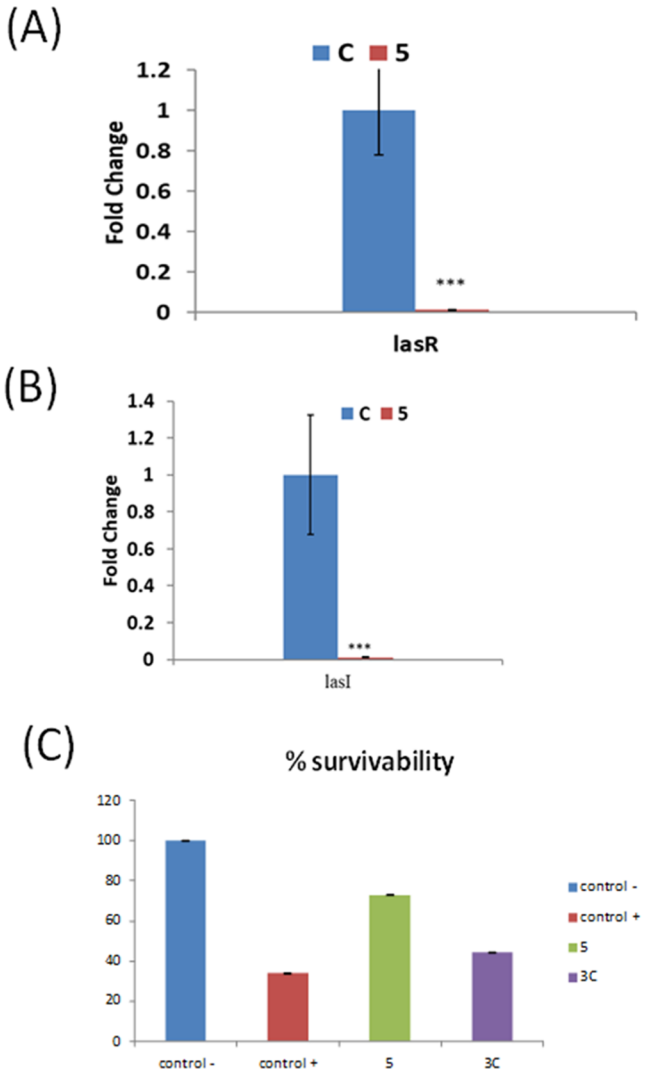

Figure 6. Effect of peptide **5** on expression of (A) lasR and (B) lasI genes and (C) % of viable cells in HEK293T cells in the presence of peptides **3c** and **5**.

dramatically increased viability. Around 72.9% ($p < 0.0001$) of PA14-infected cells survived in the presence of the compound. In the literature, the phase contrast microscopic studies have been explored to visualize morphology (the shape and size) of bacteria which are directly related to their membrane.[32] Thus, we planned to study the impact of peptide **5** in the bacteria membrane by phase contrast microscopic techniques and compared with the control study (without peptide **5**). Their images are provided in the SI (Figure S74). We notice that the shape and size of the bacterium are unaffected with peptide **5**. These studies further support that bacterial membranes are unaffected with peptide **5**. As a result of these findings, compound **5** (40 μM) may be useful as a biofilm, swarming, pyocyanin, and virulence inhibitor in acute PA infections.

We successfully synthesized the rationally designed salicylic and polyamine-conjugated peptides. Their structures and confirmations in the solution phase are demonstrated by NMR, while their solid-state structures are confirmed by single-crystal X-ray studies. A few of them form a supramolecular unique self-assembly structure. Interestingly, their packing diagram exhibit unique structures such as helix, β turn, and cross-linking. Our biochemical studies reveal that one of conjugated peptides is a quorum sensing inhibitor.

EXPERIMENTAL SECTION

Materials and Instrumentation. Except as otherwise specified, all commercial reagents were used without further purification. Natural and unnatural amino acids, salicylic acid, picolylamine, DIPA, NMM, EDC.HCl, and HOBt were purchased from Spectrochem and Sigma-Aldrich. Anhydrous DMF was purchased from Merck. Reactions were carefully monitored by thin-layer chromatography (TLC) and visualized under UV or by performing a ninhydrin test. Silica gel column chromatography was carried out on Merck silica gel 100−200 mesh. Nuclear magnetic resonance (NMR) spectra were recorded on a Bruker 400 MHz spectrometer operating at 400 and 101 MHz for ^{1}H and ^{13}C acquisitions, respectively. Chemical shifts for ^{1}H and ^{13}C are reported in ppm downfield from tetramethyl silane as an internal standard. Data are abbreviated as follows: s = singlet, d = doublet, t = triplet, q = quartet, quin = quintet, m = multiplate, and br = broad. All HRMS data were recorded with a Bruker MicroTOF-Q II spectrometer

General Procedure for Peptide Synthesis. *Synthesis of Salicylic Acid-Derivatized Peptides.* Salicylic acid/salicylic acid-derivatized L-amino acid (1 equiv) was dissolved in commercially purchased anhydrous DMF, followed by addition of NMM (3 equiv). Resulting solution was cooled to 0 °C, and EDC.HCl (1.2 equiv) was added, followed by addition of HOBt (1.2 equiv) and L-methylated amino acid. Then, the reaction mixture is removed from the ice bath and placed in a preheated heating bath at 55 °C for 8 h. After completion, the reaction mixture is concentrated under reduced pressure and extracted three times in water and ethyl acetate. The organic layer is dried over sodium sulfate and concentrated. The concentrated crude mixture is purified by column chromatography with organic solvent system EtOAc and hexane and characterized by ^{1}H, ^{13}C NMR and ESI-HRMS techniques. Hydrolysis of salicylic acid-derivatized L-amino acid methyl ester is performed by 1N LiOH over 8 h.

Coupling of Picolylamine. Salicylic acid-derivatized L-amino acid (1 equiv) was dissolved in commercially purchased anhydrous, DMF followed by addition of di-isopropyl amine (DIPA) (1.5 equiv). Resulting solution was cooled to 0 °C, and EDC.HCl (1.2 equiv) was added, followed by addition of HOBt (1.2 equiv) and picolylamine (1.2 equiv). The reaction mixture is stirred overnight at 55 °C. After completion, the reaction mixture is concentrated under reduced pressure and extracted three times in ethyl acetate and water. The organic layer is dried over sodium sulfate and concentrated. The concentrated crude mixture is purified by column chromatography with organic solvent system EtOAC and MeOH and characterized by ^{1}H, ^{13}C NMR and ESI-HRMS techniques.

*Methyl (2-Hydroxybenzyol) Glycinate (**2a**).* Compound **2a** was synthesized by the abovementioned procedure and purified by column chromatography with solvent system ethyl acetate/hexane (12:88) as a colorless gummy compound (86% yield). ^{1}H NMR (400 MHz, CDCl3) δ (ppm) 12.01 (s, 1H), 7.46 (d, J = 8.0 Hz, 1H), 7.40 (t, J = 7.7 Hz, 1H), 7.06 (s, 1H), 6.96 (d, J = 12.0 Hz, 1H), 6.85 (t, J = 7.5 Hz, 1H), 4.22 (d, J = 4.0 Hz, 2H), 3.82(s,3H). ^{13}C NMR (101 MHz, CDCl3) δ (ppm) 170.4, 170.1, 161.4, 134.6, 125.8, 118.9, 118.6, 113.7, 52.7, 41.2. HRMS (ESI-TOF) m/z: $[M + Na]^{+}$ calcd. For $C_{10}H_{11}NO_4Na$ 232.0586, observed 232.0600.

https://doi.org/10.1021/acsomega.3c03404
ACS Omega 2023, 8, 30349−30358

Methyl (2-Hydroxybenzoyl)-L-alaninate ***(2b)***. Compound **2b** was synthesized by the abovementioned procedure and purified by column chromatography with solvent system ethyl acetate/hexane (15:85) as a white solid (84% yield). ^{1}H NMR (400 MHz, CDCl3) δ (ppm) 12.09 (s, 1H), 7.44 (d, J = 8.0 Hz, 1H), 7.38 (t, J = 7.7 Hz, 1H), 7.10 (s, 1H), 6.94 (d, J = 8.3 Hz, 1H), 6.83 (t, J = 7.6 Hz, 1H), 4.78 (dd, J = 14.3, 7.1 Hz, 1H), 3.80 (s, 3H), 1.52 (d, J = 4.0 Hz, 3H). 13 C NMR (101 MHz, CDCl3) δ (ppm) 173.5, 169.5, 161.5, 134.5, 125.8, 118.8, 118.5, 113.8, 52.8, 48.2, 18.3. HRMS (ESI-TOF) m/z: $[M + Na]^+$ calcd. For $C_{11}H_{13}NO_4Na$ 246.0737, observed 246.0733.

Methyl (2-Hydroxybenzoyl)-L-valinate ***(2c)***. Compound **2c** was synthesized by the abovementioned procedure and purified by column chromatography with solvent system ethyl acetate/hexane (12:88) as a white solid (83% yield). ^{1}H NMR (700 MHz, CDCl3) δ (ppm) 12.05 (s, 1H), 7.51−7.47 (m, 1H), 7.42−7.37 (m, 1H), 6.93−6.91 (m, 1H), 6.89−6.84 (m, 2H), 4.74 (dd, J = 8.4, 4.9 Hz, 1H), 3.79 (s, 3H), 2.29 (dd, J = 6.8, 5.0 Hz, 1H), 1.03 (dd, J = 6.8, 3.4 Hz, 6H). ^{13}C NMR (101 MHz, CDCl3) δ (ppm) 172.3, 169.8, 161.5, 134.5, 125.7, 118.8, 118.6, 113.9, 57.1, 52.5, 31.6, 18.9, 18.1. HRMS (ESI-TOF) m/z: $[M + H]^+$ calcd. For $C_{13}H_{18}NO_4$ 252.1236, observed 252.1223.

Methyl (2-Hydroxybenzoyl)-L-leucinate ***(2d)***. Compound **2d** was synthesized by the abovementioned procedure and purified by column chromatography with solvent system ethyl acetate/hexane (10:90) as a white solid (81% yield). ^{1}H NMR (400 MHz, $CDCl_3$) δ (ppm) 12.07 (s, 1H), 7.45 (dd, J = 8.0, 1.4 Hz, 1H), 7.38−7.31 (m, 1H), 7.12 (d, J = 8.0 Hz, 1H), 6.93−6.89 (m, 1H), 6.84−6.77 (m, 1H), 4.90−4.80 (m, 1H), 3.79 (s, 3H), 1.81−1.64 (m, 3H), 0.98 (d, J = 8.0 Hz, 6H). ^{13}C NMR (101 MHz, $CDCl_3$) δ (ppm) 173.9, 169.9, 161.4, 134.5, 125.8, 118.7, 118.5, 113.7, 52.6, 50.8, 41.3, 24.9, 22.8, 21.8. HRMS (ESI-TOF) m/z: $[M + H]^+$ calcd. For $C_{14}H_{20}NO_4$ 266.1392, observed 266.1367.

2-Hydroxy-N-(2-oxo-2-((pyridine-2-ylmethyl)amino)-ethyl)benzamide ***(3a)***. Compound **3a** was synthesized by the abovementioned procedure and purified by column chromatography with solvent system ethyl acetate/methanol (98:2) as a white solid (79% yield). ^{1}H NMR (400 MHz, $CDCl_3$) δ (ppm) 12.13 (s, 1H), 8.54 (d, J = 4.6 Hz, 1H), 7.69 (t, J = 7.6 Hz, 1H), 7.52 (d, J = 8.0 Hz, 1H), 7.44 (s, 1H), 7.40 (t, J = 7.9 Hz, 1H), 7.28 (d, J = 10.5 Hz, 3H), 7.25−7.20 (m, 1H), 6.97 (d, J = 8.4 Hz, 1H), 6.86 (t, J = 7.6 Hz, 1H), 4.63 (d, J = 4.9 Hz, 2H), 4.21(d, J = 4.7 Hz, 2H). ^{13}C NMR (100.06 MHz, $CDCl_3$) δ (ppm) 170.1, 168.2, 161.5, 155.4, 149.1, 137.0, 134.5, 126.0, 122.7, 122.1, 118.9, 118.5, 113.9, 44.4, 42.8. HRMS (ESI-TOF) m/z: $[M + Na]^+$ calcd. For $C_{15}H_{15}N_3O_3Na$ 308.1006, observed 308.1003.

2-Hydroxy-N-(1-oxo-1((pyridine-2-ylmethyl)amino)-propan-2-yl)benzamide ***(3b)***. Compound **3b** was synthesized by the abovementioned procedure and purified by column chromatography with solvent system ethyl acetate/methanol (97:3) as a white solid (77% yield). ^{1}H NMR (400 MHz, $CDCl_3$) δ (ppm) 12.19 (s, 1H), 8.52 (d, J = 4.0 Hz, 1H), 7.67 (t, J = 4.0 Hz, 1H), 7.53 (d, J = 8.0 Hz, 2H), 7.46 (s, 1H), 7.37 (t, J = 8.0 Hz, 1H), 7.28−7.24 (d, J = 4.0 Hz, 1H), 7.23−7.17 (t, J = 8.0 Hz, 1H), 6.95 (d, J = 8.0 Hz, 1H), 6.82 (t, J = 8.0 Hz, 1H), 4.78 (m, 1H), 4.59 (t, J = 4.0 Hz, 2H), 1.53 (d, J = 8.0 Hz, 3H). ^{13}C NMR (101 MHz, $CDCl_3$) δ (ppm) 172.2, 169.5, 161.3, 155.8, 149.0, 137.0, 134.3, 126.3, 122.6, 122.1, 118.8, 118.3, 114.2, 48.9, 44.5, 18.9. HRMS (ESI-TOF) m/z: $[M + H]^+$ calcd. For $C_{16}H_{18}N_3O_3$ 300.1348, observed 300.1355.

2-Hydroxy-N-(3-methyl-1-oxo-1-((pyridine-2-ylmethyl)-amino)butan-2-yl)benzamide ***(3c)***. Compound **3c** was synthesized by the abovementioned procedure and purified by column chromatography with solvent system ethyl acetate/methanol (97:3) as a white solid (71% yield). $^{-1}$H NMR (400 MHz, $CDCl_3$) δ (ppm) 12.20 (s, 1H), 8.50 (d, J = 1.8 Hz, 1H), 7.87 (s, 2H), 7.63 (m, 2H), 7.36−7.31 (m, 1H), 7.30−7.27 (m, 1H), 7.18 (d, J = 1.9 Hz, 1H), 6.94 (m, 1H), 6.77 (m, 1H), 4.59 (d, J = 5.8 Hz, 3H), 2.22 (m, 1H), 1.25−0.77 (d, J = 8.0 Hz, 6H). ^{13}C NMR (101 MHz, $CDCl_3$) δ (ppm) 171.5, 169.5, 160.7, 156.2, 148.9, 136.9, 134.1, 126.9, 122.5, 122.1, 118.8, 118.1, 114.7, 58.77, 44.56, 31.29, 19.3, 18.6. HRMS (ESI-TOF) m/z: $[M + H]^+$ calcd. For $C_{18}H_{22}N_3O_3$ 328.1661, observed 328.1681.

2-Hydroxy-N-(4-methyl-1-oxo-1-((pyridin-2-ylmethylamino)pentan-2-yl)benzamide ***(3d)***. Compound **3d** was synthesized by the abovementioned procedure and purified by column chromatography with solvent system ethyl acetate/methanol (97:3) as a white solid (70% yield). ^{1}H NMR (400 MHz, $CDCl_3$) δ (ppm) 12.21 (s, 1H), 8.47 (d, J = 4.4 Hz, 1H), 8.19 (d, J = 8.0 Hz, 1H), 8.10 (q, J = 16.0 Hz, 1H), 7.66 (dd, J = 8.0, 1.3 Hz, 1H), 7.60 (t, J = 7.7 Hz, 1H), 7.33−7.24 (m, 2H), 7.15 (dd, J = 7.3, 5.1 Hz, 1H), 6.89 (d, J = 8.4 Hz, 1H), 6.70 (t, J = 7.6 Hz, 1H), 4.85 (m, 1H), 4.56 (d, J = 5.4 Hz, 2H), 1.82−1.54 (m, 3H), 0.95−0.83 (m, 6H). ^{13}C NMR (101 MHz, $CDCl_3$) δ (ppm) 172.9, 169.74, 160.73, 156.54, 148.9, 137.0, 134.1, 127.1, 122.5, 122.0, 118.8, 118.0, 114.7, 52.0, 44.7, 41.1, 24.9, 22.9, 21.9. HRMS (ESI-TOF) m/z: $[M + H]^+$ calcd. For $C_{19}H_{24}N_3O_3$ 342.1818, observed 342.1793.

Methyl (2-Hydroxybenzoyl)glycyl-L-alaninate ***(4a)***. Compound **4a** was synthesized by the abovementioned procedure and purified by column chromatography with solvent system ethyl acetate/hexane (60:40) as a white solid (79% yield). ^{1}H NMR (400 MHz, $CDCl_3$) δ (ppm) 12.03 (s, 1H), 7.49 (d, J = 7.9 Hz, 1H), 7.43−7.34 (m, 2H), 6.98 (d, J = 8.3 Hz, 1H), 6.86 (t, J = 7.6 Hz, 1H), 6.65 (s, 1H), 4.63 (m, 1H), 4.15 (d, J = 4.8 Hz, 2H), 3.77 (s, 3H), 1.47 (d, J = 7.2 Hz, 3H). ^{13}C NMR (101 MHz, $CDCl_3$) δ (ppm) 173.1, 170.2, 168.0, 161.5, 134.6, 126.0, 118.9, 118.5, 113.7, 52.7, 48.4, 42.8, 18.3. HRMS (ESI-TOF) m/z: $[M + Na]^+$ calcd. For $C_{13}H_{16}N_2O_5Na$ 303.0951, observed 303.0952.

Methyl 3-(2-(2-Hydroxybenzamido)acetamido)-propanoate ***(4b)***. Compound **4b** was synthesized by the abovementioned procedure and purified by column chromatography with solvent system ethyl acetate/hexane (65:35) as a white solid (73% yield). ^{1}H NMR (400 MHz, $CDCl_3$) δ (ppm) 12.01 (s, 1H), 7.68 (s, 1H), 7.52 (d, J = 8.0 Hz, 1H), 7.37 (t, J = 7.8 Hz, 1H), 6.94 (d, J = 8.3 Hz, 1H), 6.83 (t, J = 7.5 Hz, 2H), 4.07 (d, J = 5.0 Hz, 2H), 3.68 (s, 3H), 3.57 (q, J = 6.0 Hz, 2H), 2.58 (t, J = 6.0 Hz, 2H). ^{13}C NMR (101 MHz, $CDCl_3$) δ (ppm) 172.3, 170.3, 168.8, 161.3, 134.5, 126.2, 118.9, 118.4, 113.9, 51.9, 43.1, 35.2, 33.6. HRMS (ESI-TOF) m/z: $[M + H]^+$ calcd. For $C_{13}H_{17}N_2O_5$ 281.1137, observed 281.1131.

Methyl 4-(2-(2-Hydroxybenzamido)acetamido)butanoate ***(4c)***. Compound **4c** was synthesized by the abovementioned procedure and purified by column chromatography with solvent system ethyl acetate/hexane (65:35) as a white solid (69% yield). ^{1}H NMR (400 MHz, $CDCl_3$) δ (ppm) 12.02 (s, 1H),8.05 (m, 1H), 7.61 (d, J = 8.0 Hz, 1H), 7.36 (t, J = 7.7 Hz,

https://doi.org/10.1021/acsomega.3c03404
ACS Omega 2023, 8, 30349−30358

1H), 7.00 (m, 1H), 6.94 (d, J = 8.3 Hz, 1H), 6.83 (t, J = 7.6 Hz, 1H), 4.09 (d, J = 5.2 Hz, 2H), 3.64 (s, 3H), 3.33 (dd, J = 12.7, 6.5 Hz, 2H), 2.37 (t, J = 7.1 Hz, 2H), 1.91−1.79 (m, 2H). ^{13}C NMR (101 MHz, $CDCl_3$) δ (ppm) 174.0, 170.4, 169.4, 161.1, 134.5, 126.6, 119.0, 118.2, 114.1, 51.8, 43.2, 39.2, 31.4, 24.3. HRMS (ESI-TOF) m/z: $[M + Na]^+$ calcd. For $C_{14}H_{18}N_2O_5Na$ 317.1108, observed 317.1103.

*2-Hydroxy-N-(2-oxo-2-((pyridine-2-ylmethyl)amino)-propan-2-yl)amino)ethyl)benzamide (**5**).* Compound **5** was synthesized by the abovementioned procedure and purified by column chromatography with solvent system ethyl acetate/methanol (96:4) as a light gray solid (yield 73%). ^{1}H NMR (400 MHz, DMSO) δ (ppm) 12.14 (s, 1H), 9.05 (s, 1H), 8.49 (d, J = 4.0 Hz, 2H), 8.32 (d, J = 8.0 Hz, 1H), 7.86 (d, J = 8.0 Hz, 1H), 7.73 (t, J = 8.0 Hz, 1H), 7.40 (t, J = 8.0 Hz, 1H), 7.25 (m, 2H), 6.91 (m, 2H), 4.37 (d, J = 4.0 Hz, 3H), 3.99 (d, J = 4.0 Hz, 2H), 1.28 (d, J = 4.0 Hz, 3H). ^{13}C NMR (101 MHz, DMSO) δ (ppm) 172.8, 168.9, 168.7, 159.7, 159.0, 149.3, 137.1, 134.1, 128.9, 122.5, 121.1, 119.2, 117.7, 116.2, 48.9, 44.6, 42.8, 18.6. HRMS (ESI-TOF) m/z: $[M + H]^+$ calcd. For $C_{18}H_{21}N_4O_4$ 357.1563, observed 357.1540.

*Methyl (2-Hydroxybenzoyl)glycyl-L-alanyl Glycinate (**6a**).* Compound **6a** was synthesized by the abovementioned procedure and purified by column chromatography with solvent system ethyl acetate/hexane (75:25) as a white solid (72% yield). ^{1}H NMR (400 MHz, $MeOD_4$) δ (ppm) 7.82 (d, J = 8.1 Hz, 1H), 7.41 (t, J = 7.7 Hz, 1H), 6.92 (m, 2H), 4.48 (d, J = 7.2 Hz, 1H), 4.11 (s, 2H), 3.97 (s, 2H), 3.73 (s, 3H), 3.33 (s, 1H), 1.42 (d, J = 7.2 Hz, 3H). ^{13}C NMR (101 MHz, $MeOD_4$) δ (ppm) 174.0, 170.2, 170.1, 169.8, 159.5, 133.6, 128.1, 118.8, 116.9, 115.6, 51.23, 48.9, 42.4, 40.4, 16.5. HRMS (ESI-TOF) m/z: $[M + H]^+$ calcd. For $C_{15}H_{20}N_3O_6$ 338.1352, observed 338.1337.

*Methyl (2-Hydroxybenzoyl)glycyl-L-alanyl Phenylalaninate (**6b**).* Compound **6b** was synthesized by the abovementioned procedure and purified by column chromatography with solvent system ethyl acetate/hexane (70:30) as a white solid (69% yield). ^{1}H NMR (400 MHz, $CDCl_3$) δ (ppm) 8.08 (s, 1H), 7.74 (s, 1H), 7.60 (d, J = 8.0 Hz, 1H), 7.42 (s, 1H), 7.33 (t, J = 8.0 Hz, 1H), 7.22−7.16 (m, 4H), 7.07 (d, J = 8.0 Hz, 2H), 6.93 (d, J = 12.0 Hz, 1H), 6.79 (t, J = 8.0 Hz, 1H), 4.89−4.80 (m, 1H), 4.62−4.54 (m, 1H), 4.06 (d, J = 4.0 Hz, 2H), 3.67 (s, 3H), 3.15−3.0 (m,2H), 1.32 (d, J = 4.0 Hz, 3H). ^{13}C NMR (101 MHz, $CDCl_3$) δ (ppm) 172.5, 171.9, 170.3, 169.3, 160.9, 135.1, 134.4, 129.2, 128.5, 127.1, 126.7, 118.9, 118.2, 116.5, 114.2, 111.6, 53.5, 52.5, 49.2, 42.9, 37.7, 18.1. HRMS (ESI-TOF) m/z: $[M + Na]^+$ calcd. For $C_{22}H_{25}N_3O_6Na$ 450.1636, observed 450.1633.

*Methyl (3-(2-(2-Hydroxybenzamido)acetamido)-propanoyl)-L-alaninate (**6c**).* Compound **6c** was synthesized by the abovementioned procedure and purified by column chromatography with solvent system ethyl acetate/hexane (75:25) as a white solid (67% yield). ^{1}H NMR (400 MHz, DMSO) δ (ppm) 12.22 (s, 1H), 9.04 (t, J = 8.0 Hz, 1H), 8.32 (d, J = 8.0 Hz, 1H), 8.03 (t, J = 4.0 Hz, 1H), 7.87 (d, J = 8.0 Hz, 1H), 7.40 (t, J = 8.0 Hz, 1H), 6.91 (m, 2H), 4.26 (m, 1H), 3.88 (d, J = 4.0 Hz, 2H), 3.61 (s, 3H), 3.28 (q, J = 12.0 Hz, 2H), 2.31 (t, J = 8.0 Hz, 2H), 1.26 (d, J = 8.0 Hz, 3H). ^{13}C NMR (101 MHz, DMSO) δ (ppm) 173.7, 170.7, 169.0, 168.8, 159.9, 134.1, 128.9, 119.2, 117.7, 116.1, 52.3, 48.0, 42.8, 35.6, 35.3, 17.4. HRMS (ESI-TOF) m/z: $[M + Na]^+$ calcd. For $C_{16}H_{21}N_3O_6Na$ 374.1323, observed 374.1304.

*Methyl (4-(2-(2-Hydroxybenzamido)butanoyl-L-alanate (**6d**).* Compound **6d** was synthesized by the abovementioned procedure and purified by column chromatography with solvent system ethyl acetate/hexane (75:25) as a white solid (63% yield). ^{1}H NMR (400 MHz, DMSO) δ (ppm) 12.24 (s, 1H), 9.05 (t, J = 5.5 Hz, 1H), 8.25 (d, J = 6.9 Hz, 1H), 8.03 (t, J = 5.4 Hz, 1H), 7.87 (d, J = 7.8 Hz, 1H), 7.40 (t, J = 7.7 Hz, 1H), 6.91 (m, 2H), 4.24 (m, 1H), 3.89 (d, J = 5.5 Hz, 2H), 3.61 (s, 3H), 3.08 (q, J = 16.0 Hz, 2H), 2.12 (t, J = 7.4 Hz, 2H), 1.64 (p, J = 7.2 Hz, 2H), 1.25 (d, J = 7.3 Hz, 3H). ^{13}C NMR (101 MHz, DMSO) δ (ppm) 173.7, 172.3, 169.0, 168.7, 159.9, 134.1, 128.9, 119.2, 117.7, 116.2, 52.3, 47.9, 42.8, 38.7, 32.9, 25.7, 17.4. HRMS (ESI-TOF) m/z: $[M + Na]^+$ calcd. For $C_{17}H_{23}N_3O_6Na$ 388.1479, observed 388.1480.

*2-Hydroxy-N-(2-oxo-2-((1-oxo-1-((2-oxo-2-((pyridin-2-ylmethyl)amino)ethyl)amino)propan-2-yl)amino)ethyl)-benzamide (**7a**).* Compound **7a** was synthesized by the abovementioned procedure and purified by column chromatography with solvent system ethyl acetate/methanol (95:5) as an off-white solid (69% yield). ^{1}H NMR (400 MHz, DMSO) δ (ppm) 12.12 (s, 1H), 9.02 (t, J = 8.0 Hz, 1H), 8.46 (d, J = 4.0 Hz, 1H), 8.32 (d, J = 8.0 Hz, 2H), 8.27 (t, J = 8.0 Hz, 1H), 7.85 (d, J = 8.0 Hz, 1H), 7.70 (t, J = 8.0 Hz, 1H), 7.40 (t, J = 8.0 Hz, 1H), 7.29−7.20 (m, 2H), 6.90 (m, 2H), 4.40−4.29 (m, 3H), 3.97 (d, J = 8.0 Hz, 2H), 3.77 (t, J = 8.0 Hz, 2H), 1.24 (d, J = 4.0 Hz, 3H). ^{13}C NMR (101 MHz, DMSO) δ (ppm) 173.0, 169.4, 168.9, 168.8, 159.7, 158.8, 149.2, 137.1, 134.1, 128.9, 122.5, 121.3, 119.2, 117.7, 116.3, 48.9, 44.5, 42.6, 18.5. HRMS (ESI-TOF) m/z: $[M + Na]^+$ calcd. For $C_{20}H_{23}N_5O_5Na$ 436.1597, observed 436.0931.

*2-Hydroxy-N-(2-oxo-2-(((2S)-1-oxo-1-((1-oxo-3-phenyl-1-((pyridine-2-ylmethyl)amino)propan-2-yl)amino)propan-3-yl)amino)ethyl)benzamide (**7b**).* Compound **7b** was synthesized by the abovementioned procedure and purified by column chromatography with solvent system ethyl acetate/MeOH (96:4) as white solid (68% yield). ^{1}H NMR (400 MHz, DMSO) δ (ppm) 12.15 (s, 1H), 9.06 (t, J = 4.0 Hz, 1H), 8.50 (t, J = 8.0 Hz, 1H), 8.46 (d, J = 8.0 Hz, 1H), 8.28 (d, J = 4.0 Hz, 1H), 8.15 (d, J = 8.0 Hz, 1H), 7.87 (d, J = 8.0 Hz, 1H), 7.64 (t, J = 8.0 Hz, 1H), 7.41 (t, J = 8.0 Hz, 1H), 7.32−7.16 (m, 7H), 7.01 (d, J = 8.0 Hz, 1H), 6.92 (m, 2H), 4.55 (m, 1H), 4.41−4.25 (m, 3H), 3.95 (d, J = 4.0 Hz, 2H), 3.07 (dd, J = 12.0, 8.0 Hz, 1H), 2.89 (dd, J = 12.0, 8.0 Hz, 1H), 1.17 (d, J = 4.0 Hz, 3H). ^{13}C NMR (101 MHz, DMSO) δ (ppm) 172.5, 171.3, 168.9, 168.8, 159.6, 158.8, 149.2, 138.1, 137.1, 134.1, 129.7, 129.0, 128.6, 126.8, 122.5, 121.0, 119.3, 117.7, 116.3, 54.7, 48.8, 44.5, 42.8, 42.6, 37.8, 18.6. HRMS (ESI-TOF) m/z: $[M + Na]^+$ calcd. For $C_{27}H_{29}N_5O_5Na$ 526.2067, observed 526.2086.

*2-Hydroxy-N-(2-oxo-2-((4-oxo-4-((1-oxo-1-((pyridine-2-ylmethyl)amino)propan-2-yl)amino)butyl)amino)ethyl)-benzamide (**7c**).* Compound **7c** was synthesized by the abovementioned procedure and purified by column chromatography with solvent system ethyl acetate/MeOH (95:5) as a gray solid (61% yield). ^{1}H NMR (400 MHz, DMSO) δ (ppm) 12.22 (s, 1H), 9.05 (t, J = 5.5 Hz, 1H), 8.47 (m, 2H), 8.16 (d, J = 7.3 Hz, 1H), 8.05 (t, J = 5.5 Hz, 1H), 7.87 (d, J = 7.9 Hz, 1H), 7.75 (t, J = 7.6 Hz, 1H), 7.40 (t, J = 7.7 Hz, 1H), 7.25 (m, 2H), 7.00−6.84 (m, 2H), 4.36 (d, J = 5.8 Hz, 2H), 4.34−4.29 (m, 1H), 3.88 (d, J = 5.5 Hz, 2H), 3.33−3.28 (m, 2H), 2.34 (m, 2H), 1.25 (d, J = 7.2 Hz, 3H). ^{13}C NMR (101 MHz, DMSO) δ (ppm) 173.1, 170.7, 168.9, 168.8, 159.9, 159.0, 149.1, 137.2, 134.1, 128.9, 122.5, 121.1, 119.2, 117.7, 116.1,

https://doi.org/10.1021/acsomega.3c03404
ACS Omega 2023, 8, 30349−30358

48.9, 44.5, 42.8, 35.8, 35.6, 18.5. ESI-HRMS m/z: $[M + Na]^+$ calcd. For $C_{21}H_{25}N_5O_5Na$ 450.1748, observed 450.1942.

*2-Hydroxy-N-(2-oxo-2-((4-oxo-4-((1-oxo-1-((pyridine-2-ylmethyl)amino)propan-2-yl)amino)butyl)amino)ethyl)-benzamide (**7d**).* Compound **7d** was synthesized by the abovementioned procedure and purified by column chromatography with solvent system ethyl acetate/MeOH (95:5) as a white solid (58% yield). ^{1}H NMR (400 MHz, DMSO) δ (ppm) 12.22 (s, 1H), 9.04 (t, J = 5.4 Hz, 1H), 8.46 (m, 2H), 8.04 (m, 2H), 7.87 (d, J = 8.0 Hz, 1H), 7.73 (t, J = 8.0 Hz, 1H), 7.40 (t, J = 8.0 Hz, 1H), 7.24 (m, 2H), 6.90 (t, J = 8.0 Hz, 2H), 4.35 (d, J = 8.0 Hz, 2H), 4.30 (t, J = 8.0 Hz, 1H), 3.89 (d, J = 8.0 Hz, 2H), 3.20−2.98 (m, 2H), 2.15 (t, J = 7.3 Hz, 2H), 1.64 (m, 2H), 1.24 (d, J = 4.0 Hz, 3H). ^{13}C NMR (101 MHz, DMSO) δ (ppm) 173.2, 172.2, 168.7, 159.9, 159.1, 149.2, 137.1, 134.1, 128.9, 122.5, 121.1, 119.2, 117.7, 48.8, 44.5, 42.8, 33.0, 25.8, 18.6, 0.6. HRMS (ESI-TOF) m/z: $[M + Na + H]^+$ calcd. For $C_{22}H_{29}N_5O_5Na$ 465.1988, observed 465.1974.

■ ASSOCIATED CONTENT

Supporting Information

The Supporting Information is available free of charge at https://pubs.acs.org/doi/10.1021/acsomega.3c03404.

^{1}H/^{13}C NMR, HRMS, and 2D-NMR (COSY and NOESY) spectra; crystal structure of peptides; DMSO-d_6 titration experiment spectra; and X-ray data of peptide derivatives (**3a**, **3b**, **3d**, **4a**, **4c**, and **5**) (PDF)

Crystallographic data 1 (CIF)

Crystallographic data 2 (CIF)

Crystallographic data 3 (CIF)

Crystallographic data 4 (CIF)

Crystallographic data 5 (CIF)

Crystallographic data 6 (CIF)

■ AUTHOR INFORMATION

Corresponding Author

Nagendra K. Sharma − *School of Chemical Sciences, National Institute of Science Education and Research (NISER), Bhubaneswar 752050 Odisha, India; Homi Bhabha National Institute, Training School Complex, Mumbai 400094, India;* orcid.org/0000-0003-0901-0523; Phone: 91-0674-249-4141/4168; Email: nagendra@niser.ac.in

Authors

Subhashree S. Panda − *School of Chemical Sciences, National Institute of Science Education and Research (NISER), Bhubaneswar 752050 Odisha, India; Homi Bhabha National Institute, Training School Complex, Mumbai 400094, India*

Supriya Kumari − *School of Chemical Sciences, National Institute of Science Education and Research (NISER), Bhubaneswar 752050 Odisha, India; School of biological Sciences, National Institute of Science Education and Research (NISER), Bhubaneswar 752050 Odisha, India*

Manjusha Dixit − *School of biological Sciences, National Institute of Science Education and Research (NISER), Bhubaneswar 752050 Odisha, India; Homi Bhabha National Institute, Training School Complex, Mumbai 400094, India;* orcid.org/0000-0002-6997-1054

Complete contact information is available at: https://pubs.acs.org/10.1021/acsomega.3c03404

Notes

The authors declare no competing financial interest.

■ ACKNOWLEDGMENTS

The authors thank SERB-New Delhi (Govt. of India, New Delhi) for the CRG grant with number CRG/2020/001028.

■ REFERENCES

(1) Raskin, I. Role of salicylic acid in plants. *Annu. Rev. Plant. Physiol. Plant. Mol. Biol.* **1992**, *43*, 439−463.

(2) Bindu, S.; Mazumder, S.; Bandyopadhyay, U. Non-steroidal anti-inflammatory drugs (NSAIDs) and organ damage: A current perspective. *Biochem. Pharmacol.* **2020**, *180*, No. 114147.

(3) Babhair, S. A.; Al-Badr, A. A.; Aboul-Enein, H. Y. Salicylamide. In *Analytical Profiles of Drug Substances*; Elsevier, 1984; Vol. *13*, pp 521−551.

(4) Nishiya, T.; Yamauchi, S.; Hirota, N.; Baba, M.; Hanazaki, I. Fluorescence studies of intramolecularly hydrogen-bonded o-hydroxyacetophenone, salicylamide, and related molecules. *J. Phys. Chem. A* **1986**, *90*, 5730−5735.

(5) Catalan, J.; Toribio, F.; Acuna, A. Intramolecular hydrogen bonding and fluorescence of salicylaldehyde, salicylamide, and o-hydroxyacetophenone in gas and condensed phase. *J. Phys. Chem. A* **1982**, *86*, 303−306.

(6) Song, Q.; Li, Y.; Cao, Z.; Qiang, X.; Tan, Z.; Deng, Y. Novel salicylamide derivatives as potent multifunctional agents for the treatment of Alzheimer's disease: Design, synthesis and biological evaluation. *Bioorg. Chem.* **2019**, *84*, 137−149.

(7) Stavropoulos, G.; Magafa, V.; Liakopoulou-Kyriakides, M.; Sinakos, Z.; Aaberg, A. Synthesis of salicyl-peptides and their effect on human platelet aggregationin vitro. *Amino Acids* **1997**, *13*, 171.

(8) Sarigiannis, Y. M.; Stavropoulos, G. P.; Liakopoulou-Kyriakides, M. T.; Makris, P. E. Novel synthetic RGD analogs incorporating salicylic acid derivatives show antiplatelet activity in vitro. *Lett. Pept. Sci* **2002**, *9*, 101−109.

(9) Montalvo, G. L.; Zhang, Y.; Young, T. M.; Costanzo, M. J.; Freeman, K. B.; Wang, J.; Clements, D. J.; Magavern, E.; Kavash, R. W.; Scott, R. W.; Liu, D.; DeGrado, W. F. De Novo Design of Self-Assembling Foldamers That Inhibit Heparin−Protein Interactions. *ACS Chem. Biol.* **2014**, *9*, 967−975.

(10) Yan, Y.; Qin, B.; Shu, Y.; Chen, X.; Yip, Y. K.; Zhang, D.; Su, H.; Zeng, H. Helical organization in foldable aromatic oligoamides by a continuous hydrogen-bonding network. *Org. Lett.* **2009**, *11*, 1201−1204.

(11) Montalvo, G. L. Foldamers: Design, synthesis, and characterization of non-natural peptides with diverse backbones, 2012.

(12) Imramovský, A.; Jorda, R.; Pauk, K.; Řezníčková, E.; Dušek, J.; Hanusek, J.; Kryštof, V. Substituted 2-hydroxy-N-(arylalkyl) benzamides induce apoptosis in cancer cell lines. *Eur. J. Med. Chem.* **2013**, *68*, 253−259.

(13) Kirin, S. I.; Dübon, P.; Weyhermüller, T.; Bill, E.; Metzler-Nolte, N. Amino acid and peptide bioconjugates of copper (II) and zinc (II) complexes with a modified N, N-bis (2-picolyl) amine ligand. *Inorg. Chem.* **2005**, *44*, 5405−5415.

(14) Pantalon Juraj, N.; Muratović, S.; Perić, B.; Šijaković Vujičić, Na.; Vianello, R.; Žilić, D.; Jagličić, Z.; Kirin, S. k. I. Structural Variety of Isopropyl-bis (2-picolyl) amine Complexes with Zinc (II) and Copper (II). *Cryst. Growth Des.* **2020**, *20*, 2440−2453.

(15) Darshani, T.; Thushara, N.; Weerasuriya, P.; Fronczek, F. R.; Perera, I. C.; Perera, T. Fluorescent di-(2-picolyl) amine based drug-like ligands and their Re (CO) 3 complexes towards biological applications. *Polyhedron* **2020**, *185*, No. 114592.

(16) Cui, S.; Liu, G.; Pu, S.; Chen, B. A highly selective fluorescent probe for Zn2+ based on a new photochromic diarylethene with a di-2-picolylamine unit. *Dyes Pigm.* **2013**, *99*, 950−956.

(17) Dotto, C.; Lombarte Serrat, A.; Ledesma, M.; Vay, C.; Ehling-Schulz, M.; Sordelli, D. O.; Grunert, T.; Buzzola, F. Salicylic acid stabilizes Staphylococcus aureus biofilm by impairing the agr quorum-sensing system. *Sci. Rep.* **2021**, *11*, No. 2953.
(18) Miller, M. B.; Bassler, B. L. Quorum sensing in bacteria. *Annu. Rev. Microbiol.* **2001**, *55*, 165−199.
(19) Alonso, B.; Fernández-Barat, L.; Di Domenico, E. G.; Marín, M.; Cercenado, E.; Merino, I.; de Pablos, M.; Muñoz, P.; Guembe, M. Characterization of the virulence of *Pseudomonas aeruginosa* strains causing ventilator-associated pneumonia. *BMC Infect. Dis.* **2020**, *20*, 1−8.
(20) Privalsky, T. M.; Soohoo, A. M.; Wang, J.; Walsh, C. T.; Wright, G. D.; Gordon, E. M.; Gray, N. S.; Khosla, C. Prospects for antibacterial discovery and development. *J. Am. Chem. Soc.* **2021**, *143*, 21127−21142.
(21) Rosenthal, V. D.; Al-Abdely, H. M.; El-Kholy, A. A.; AlKhawaja, S. A. A.; Leblebicioglu, H.; Mehta, Y.; Rai, V.; Hung, N. V.; Kanj, S. S.; Salama, M. F.; et al. International Nosocomial Infection Control Consortium report, data summary of 50 countries for 2010-2015: Device-associated module. *Am. J. Infect. Control* **2016**, *44*, 1495−1504.
(22) Lambert, M.-L.; Suetens, C.; Savey, A.; Palomar, M.; Hiesmayr, M.; Morales, I.; Agodi, A.; Frank, U.; Mertens, K.; Schumacher, M.; Wolkewitz, M. Clinical outcomes of health-care-associated infections and antimicrobial resistance in patients admitted to European intensive-care units: a cohort study. *Lancet Infect. Dis.* **2011**, *11*, 30−38.
(23) Choi, H.; Ham, S.-Y.; Cha, E.; Shin, Y.; Kim, H.-S.; Bang, J. K.; Son, S.-H.; Park, H.-D.; Byun, Y. Structure−activity relationships of 6- and 8-gingerol analogs as anti-biofilm agents. *J. Med. Chem.* **2017**, *60*, 9821−9837.
(24) Meher, S.; Kumari, S.; Dixit, M.; Sharma, N. K. Cu-Catalyzed Synthesis of Alkylaminotroponyl Sulfones as *Pseudomonas Aeruginosa* Quorum Sensing Inhibitors Targeting lasI/R QS Circuitry. *Chem. - Asian J.* **2022**, *17*, No. e202200866.
(25) Dalabehera, N. R.; Meher, S.; Bhusana Palai, B.; Sharma, N. K. Instability of amide bond with trifluoroacetic acid (20%): synthesis, conformational analysis, and mechanistic insights into cleavable amide bond comprising β-troponylhydrazino acid. *ACS omega* **2020**, *5*, 26141−26152.
(26) Gupta, M. K.; Jena, C. K.; Balachandra, C.; Sharma, N. K. Unusual Pseudopeptides: Syntheses and Structural Analyses of Ethylenediprolyl Peptides and Their Metal Complexes with Cu (II) Ion. *J. Org. Chem.* **2021**, *86*, 16327−16336.
(27) Kearns, D. B. A field guide to bacterial swarming motility. *Nat. Rev. Microbiol.* **2010**, *8*, 634−644.
(28) Chuang, S. K.; Vrla, G. D.; Fröhlich, K. S.; Gitai, Z. Surface association sensitizes *Pseudomonas aeruginosa* to quorum sensing. *Nat. Commun* **2019**, *10*, No. 4118.
(29) Dietrich, L. E. P.; Price-Whelan, A.; Petersen, A.; Whiteley, M.; Newman, D. K. The phenazine pyocyanin is a terminal signalling factor in the quorum sensing network of *Pseudomonas aeruginosa*. *Mol. Microbiol.* **2006**, *61*, 1308−1321.
(30) Hurley, M. N.; Cámara, M.; Smyth, A. R. Novel approaches to the treatment of *Pseudomonas aeruginosa* infections in cystic fibrosis. *Eur. Respir. J.* **2012**, *40*, 1014−1023.
(31) Jayaseelan, S.; Ramaswamy, D.; Dharmaraj, S. Pyocyanin: production, applications, challenges and new insights. *World J. Microbiol. Biotechnol.* **2014**, *30*, 1159−1168.
(32) Reshes, G.; Vanounou, S.; Fishov, I.; Feingold, M. Cell shape dynamics in Escherichia coli. *Biophys. J.* **2008**, *94*, 251−264.

https://doi.org/10.1021/acsomega.3c03404
ACS Omega 2023, 8, 30349−30358